VOLUME 81 PAPER No. 813

PROCEEDINGS

AMERICAN SOCIETY
OF
CIVIL ENGINEERS

OCTOBER, 1955

DISCUSSION OF PROCEEDINGS PAPERS

544, 558, 583, 663

STRUCTURAL DIVISION

Copyright 1955 by the American Society of Civil Engineers
Printed in the United States of America

Headquarters of the Society
33 W. 39th St.
New York 18, N. Y.

PRICE $0.50 PER COPY

Current discussion of papers sponsored by the Structural Division is presented as follows:

Number Page

544 Examples of Timber Structure Failures, by Michael N. Salgo. (November, 1954. Prior discussion: 589, 701. Discussion closed)

Salgo, Michael N. (Closure) 1

558 An Influence Line Analysis for Suspension Bridges, by David J. Peery. (December, 1954. Prior discussion: 701. Discussion closed)

Peery, David J. (Closure) 3

583 Ultimate Slopes and Deflections—A Brief for Limit Design, by George C. Ernst. (January, 1955. Prior discussion: 765. Discussion closed)

Ernst, George C. (Closure) 17

663 Lateral Bending of Suspension Bridges, by Cevdet A. Erzen. (April, 1955. Prior discussion: None. Discussion closed)

Selberg, A. 23
Erzen, Cevdet A. (Closure) 24

Reprints from this publication may be made on condition that the full title of paper, name of author, page reference (or paper number), and date of publication by the Society are given.

The Society is not responsible for any statement made or opinion expressed in its publications.

This paper was published at 1745 S. State Street, Ann Arbor, Mich., by the American Society of Civil Engineers. Editorial and General Offices are at 33 West Thirty-ninth Street, New York 18, N.Y.

Discussion of
"EXAMPLES OF TIMBER STRUCTURE FAILURES"

by Michael N. Salgo
(Proc. Paper 544)

MICHAEL N. SALGO,[1] M. ASCE.—Dr. Stern, in his discussion, inquires as to the type of split rings, flat face, bevelled on inner or both faces, for the structures reported on. All of the structures reported on had the standard split ring in use at that time namely, the split ring with a bevelled inside and flat outside face. In view of this, the desired information on field experiences with flat sided versus bevelled split ring connectors is not available from the writer.

Mr. Gloss, in his discussion, sets forth some of his experiences and raises certain questions. Comments on these will be set forth in subsequent paragraphs.

Mr. Gloss apparently is of the opinion that the paper and parts of the conclusion may be construed as placing the blame for failures encountered on truss types or fastening means, rather than on the errors of design, fabrication or maintenance. This was definitely not the intent of the paper. Quite the contrary, the writer took particular care, in discussing the failures, to point out the respective causes which were basically design and/or construction and/or maintenance. Certain types of framing did have higher incidence of failures than others and these were pointed out.

As Mr. Gloss indicates, the writer is of the opinion that the over-all performance record of timber trusses during World War II was outstanding and, as stated in the paper, "the availability and use of long-span timber structures during World War II is considered to have been a major contribution to the war effort." However, failures and difficulties did occur and from these certain lessons can be learned.

One of the major sources of difficulties with parallel chord trusses during World War II was the fact that actual deflections were considerably in excess of that which could have been predicted on the basis of available design data for deformation of split ring joints under load. Subsequent design data, as promulgated, increased the expected deflections for timber connector type trusses. However, by this time, many timber truss structures had been built. Results of this manifested itself in such items as lack of clearance for bridge cranes, binding of large hangar doors, etc. These structures were cambered on the basis of the then available design data. Where bowstring trusses were used, the effect of the deformation data was not as critical as in the parallel chord trusses.

Mr. Gloss indicates particular interest in the discussion of secondary stresses. Although recognizing the presence of the secondary stresses, he questions the validity of most computations to determine their magnitude, since such computations involve many critical assumptions. It is the writer's opinion that the assumptions are not necessarily as critical as Mr. Gloss sets forth, since the same assumptions that satisfactorily predict the total deflections (including creep effects) can also be used to predict member distress. Figure 19 illustrated the results of such an analysis, which were subsequently used as the basis for necessary repairs and strengthening. However, these analyses are often quite difficult, time consuming, and beyond capabilities of ordinary design procedures; for this reason, inclusion of certain limiting factors in building codes are considered warranted.

---

[1] Principal Asst. to Dist. Civ. Eng., Third Naval Dist. Headquarters, New York, N. Y.

There appears to be an honest difference of professional opinion concerning the proposed restrictions for trusses other than bowstring where unseasoned lumber is to be used. To further belabor this point at this time does not appear warranted. However, at the time this paper was formally presented at the Annual New York Convention of the ASCE on October 21, 1953, the inclusion of the proposed restrictions was still pending. A decision was subsequently made not to have the restrictions in the AITC-Timber Construction Standards. The writer, however, still considers it to be good practice and so recommends.

In closing, the writer wishes to restate the basic purpose of the paper which was to present certain actual observed experiences, particularly with reference to data on failures of timber structures observed, from which certain lessons can be learned; and the final conclusion that "TIMBER STRUCTURES PROPERLY DESIGNED, CONSTRUCTED, AND MAINTAINED HAVE TAKEN THEIR PLACE AS MAJOR COMPONENTS IN OUR PRESENT DAY CONSTRUCTION PROGRAM."

Discussion of
"AN INFLUENCE LINE ANALYSIS FOR SUSPENSION BRIDGES"

by David J. Peery
(Proc. Paper 558)

DAVID J. PEERY,[1] M. ASCE.—The discussions include significant supplementary theory, as well as substantiation of the writer's basic influence line procedures. The contributions of the discussers are appreciated. Most of the discussions treat the simpler case of the bridge with hinged stiffening trusses. The obvious questions concern the accuracy and the relative simplicity of the influence line procedure, as compared with the customary deflection theory.

Mr. Sih questions whether the influence lines are applicable to unstiffened bridges, and feels that they give a "misleading concept of the function of the stiffening truss." The influence lines shown in Fig. 16 include the complete range of values from $c\ell = 0$ (elastic theory) to $c\ell = \infty$ (unstiffened bridge). These influence lines are readily visualized as deflection curves, whereas the conventional long equations of exponential or hyperbolic terms do not present a simple physical picture.

Mr. Sih also questions the assumption of superposition. In reality, this assumption is identical with that used in all deflection theory analysis, and influence line ordinates can be calculated to any desired degree of precision, by successive corrections of the $c\ell$ values. The basic differential equation of the deflection theory, $\eta'' - c^2\eta = -M/EI$ is non-linear, since c is not constant. It is not feasible to integrate this non-linear equation, so c is always assumed constant during integration, thus linearizing the differential equation. Superposition procedures apply for solution of linear differential equations, but not for non-linear problems.

Dr. Karol presents simple equations for the variation of H, M, and V with $c\ell$. When these equations are used, it is necessary to calculate influence lines for only one value of $c\ell$. Values can then be corrected to correspond to the true value of $c\ell$ for each particular loading. The computation work is obviously reduced from that required to calculate two sets of influence lines.

Mr. Paulbaum extends the influence line procedure to the calculation of shears in the stiffening truss. This is an important contribution, since two segments of the span may be loaded and the influence lines provide the only convenient method for finding the correct loaded length.

Professor Franciosi substantiates the author's procedure of finding influence lines as deflection curves, or by using the theorem of Betti. He proves the validity of this procedure for suspension bridges and arches, provided H_R remains constant. He also proposes a method of successive approximation, which is applicable to arches or suspension bridges. The successive approximations would probably converge more slowly for suspension bridges than for arches because of the higher values of $c\ell$. The equations for M are also more sensitive to changes in $c\ell$ than are the equations for H.

---

[1] Prof. of Aeronautical Eng., Univ. of Michigan, Ann Arbor, Mich.

Several of the discussers requested more design data and further examples of the computational procedure. Charts and tables will therefore be presented for bridges with simply supported trusses. Most bridges of this type are somewhat similar, with most of the flexibility contributed by the main span. The side spans are always considered as unloaded or as uniformly loaded for the entire span; hence, influence lines are not required for the side spans. It will be assumed that 80 percent of the denominator D of the H-equation (Eqs. 12 and 13) is contributed by the main span term, which will be designated as D_o, and the remaining 20 percent of D is contributed by the side span terms $2D_s$ and the cable stretch term $\frac{L_s}{AE_c}$. This assumption is stated in the following equations, which also define D_o and D_s.

$$D = D_o + 2D_s + \frac{L_s}{AE_c} \tag{62}$$

$$D \cong 1.25\, D_o \tag{63}$$

$$D_o = -\frac{8f}{\ell^2}\int_o^{\ell} \eta_h dx \tag{64}$$

$$D_s = -\frac{8f_1}{\ell_1^2}\int_o^{\ell_1} \eta_{h_1} dx \tag{65}$$

The influence lines will be calculated for bridges with these proportions. The final bending moments will then be corrected to the true ratios of D/D_o.

The value of D_o (or D_s) is obtained by substituting η_h from Eq. 11 into Eq. 64, and integrating.

$$D_o = \frac{64\, f^2\, \ell}{EI\, c^2 \ell^2}\left[\frac{1}{12} - \frac{1}{c^2\ell^2} + \frac{2\tanh c\ell/2}{c^3\ell^3}\right] \tag{66}$$

For conversion to exponentials, $\tanh c\ell/2 = (e^{c\ell} - 1)/(e^{c\ell} + 1)$. Values of $D_oEI/f^2\ell$ or $D_sEI_1/f_1^2\,\ell_1$ are listed in Table 6 for various values of $c\ell$. These terms are also multiplied by $c^2\ell^2$ in order to permit easy interpolation at the higher values of $c\ell$.

The H-influence line is now obtained by substituting $D=1.25\, D_o$, and values of η_h from Eq. 11 into Eq. 13. The H-influence lines for $\ell = 10f$ are plotted in Fig. 16 for various values of $c\ell$. The H-influence lines are seen to have little variation in shape, since the maximum ordinate varies from 1.5625 for $c\ell = 0$ to 1.5000 for $c\ell = \infty$, or only 4 percent. This confirms Dr. Karol's statement that the H-influence lines are affinely related. For other ratios of f/ℓ and D/D_o, the H ordinates should be multiplied by $\ell/10f \times 1.25\, D_o/D$. Dr. Karol's Eq. 27 depends on a typical variation of the ratio D_o/D with $c\ell$. The values of H decrease with higher values of $c\ell$, since the ratio D_o/D decreases. This effect is not shown in Fig. 16, which shows only the relative shapes of the H-influence lines.

For a uniformly distributed live-load p extending a distance k' from the left end of the span, the values of $H/p\ell$ are obtained from the areas under the H-influence lines. These values are shown in Table 7. For live loads over the right side from k' to ℓ, the values in Table 7 may be subtracted from 1.000, since $H/p\ell = 1.000$ for a full live load. Any partial live loading may be considered by superposition.

Values of m_h/f may be calculated from Eq. 10. For convenient interpolation, these values are multiplied by $c^2\ell^2$ and listed in Table 8. The values of m_p obtained from Eqs. 8 and 9 depend only on $c\ell$. The values of m_h vary directly with the sag f, and the values of H vary inversely with f. The product Hm_h is therefore independent of f, and varies only with $c\ell$, when $D = 1.25\ D_o$. Consequently, the bending moment influence lines may be calculated from Eq. 14 as functions of $c\ell$ only, if D is assumed equal to $1.25\ D_o$. These bending moment influence lines are plotted in Figs. 16 to 18. For normal ratios of $\frac{D}{D_o}$, the influence lines of Figs. 16 to 18 are sufficiently accurate to determine the final load position for maximum positive or negative bending moment.

The positive and negative areas under the influence lines of Figs. 16 to 18 may be calculated by integration of Eqs. 8, 9, and 11. These values are plotted as $c\ell \times M/p\ell^2$ in Figs. 19 and 20. The factor $c\ell$ is included so that the curves may be plotted to a larger scale.

The bending moments calculated for $D/D_o = 1.25$ must now be corrected to the true ratio of D/D_o. If the value from Table 7 is designated as H_o, the increment δH produces a bending moment correction of $\delta H \times m_h$.

$$\delta H = H_o \left(\frac{1.25\ D_o}{D} - 1\right) \frac{\ell}{10f} \tag{67}$$

This value of δH may be added to H_t to correct the positive main span bending moments.

$$M = (H_t + \delta H)m_h \tag{68}$$

The maximum negative bending moments occur when the side spans are fully loaded. A full live load in one side span produces a cable component which is designated by H_s. The negative bending moments in the main span have the following correction:

$$M = (2H_s + H_t + \delta H)m_h \tag{69}$$

The cable component for full live load in one side span is obtained by integrating Eq. 13 over one side span and substituting D_s from Eq. 65. The value $H_w = w_1\ell_1{}^2/8\ f_1$ is also substituted.

$$H_s = H_w \frac{P}{w_1} \frac{D_s}{D} \tag{70}$$

The side span bending moments, M_s, are calculated directly from Eq. 10. For negative bending moments in one side span, the value of H is calculated for the other spans loaded at minimum temperature.

$$M = Hm_h \tag{71}$$

For positive bending moment in one side span, only that span is loaded at maximum temperature. The uniform load p produces a moment proportional to the moment m_h by the ratio $-\frac{p\ell_1{}^2}{8f_1}$ or $-H_w \frac{P}{w_1}$. The total positive bending moment is

$$M = (-H_w \frac{p}{w_1} + H_s - H_t)\ m_h \tag{72}$$

The values of m_h can be interpolated from Table 8.

Numerical Application

The following structure will be analyzed. The dimensions are $\ell = 3800$ ft, $\ell_1 = 1800$ ft, $f = 350$ ft, $f_1 = 78.53$ ft, $L_s = 9140$ ft and $L_t = 8482$ ft. The flexibility properties for one side are $EI = EI_1 = 1884 \times 10^6$ ft^2 kips, and $L_s/A\,E_c = 0.000880$ ft/kip. The load per cable is $w = w_1 = 4.7$ kip/ft and $p = 1.0$ kip/ft. The values $t = \pm\, 60^{\circ}$F, $\omega = 0.0000065$ and $H_w = w\ell^2/8f = 24{,}240$ kips are used.

The main span bending moments will be interpolated between calculated values for $c\ell = 14$ and $c\ell = 15$, but only the calculations for $c\ell = 14$ are shown. For $c\ell = 14$, $c_1\ell_1 = 14 \times 1800/3800 = 6.63$, and $H_r = c^2EI = 25{,}570^K$. From Table 6, $D_o = 5.053\, f^2/H_r\,\ell = 0.006370$, and $D_s = 4.314 \times f_1{}^2/H_r\,\ell_1 = 0.000578$. From Eq. 62, $D = 0.008406$ ft/kip. The ratio D/D_o is 1.320. For a temperature change, $H_t = \pm\,\omega t L_t/D = \pm\, 393$ kips. For full live load in the main span, $H = H_w \dfrac{p}{w}\, \dfrac{D_o}{D} = 3908^K$. For full live load in one side span, $H_s = H_w \dfrac{p}{w_1}\, \dfrac{D_s}{D} = 354^K$. Maximum $H = 3908 + 2 \times 354 + 393 = 5009$ kips.

The bending moments are calculated in Table 9. The load positions are obtained from the influence lines. The main-span bending moments are first obtained from Figs. 19 and 20, which represent the positive and negative areas under the influence lines. These moments are designated as M_i in lines 5 and 11 of Table 9. The moments are then corrected for the D/D_o ratio, and for temperature and side span loads. The moments calculated in lines 7 and 13 are for $c\ell = 14$. The moments shown in lines 8 and 14 are interpolated from similar calculations for $c\ell = 15$. The side span bending moments are calculated for the correct values of $c_1\ell_1$ in lines 16 and 18.

SUMMARY

The original paper presented methods for obtaining influence lines for suspension bridges with any number of spans, and with hinged or continuous stiffening trusses. The procedure permits a direct determination of the critical loading conditions, and permits consideration of any type of live load distribution, without the usual restriction of uniform loading. Influence lines are obtained by superimposing simple deflection curves, thus permitting a designer to detect gross errors. The customary long, abstract equations are avoided. Any desired degree of accuracy may be obtained by calculating influence lines at small intervals of $c\ell$, although engineering accuracy may always be obtained with only two values of $c\ell$

For two-hinged suspension bridges, influence line procedures had previously been used by Rode,[4] Selberg,[5] Asplund,[6] and Karol,[7] all of whom prepared tabular data. Similar charts and curves are readily prepared for continuous bridges since the equations (18 and 19) are simple. However, tables covering the complete range of values appear too voluminous for this paper.

The influence lines constructed for $D = 1.25\, D_o$ appear adequate for most two-hinged bridges. For bridges of unusual proportions, the influence lines may be easily corrected to give the exact load position. Similar influence lines may be constructed for shears.

Acknowledgment: The data used in the numerical application correspond to preliminary dimensions of the Mackinac Straits Bridge, and were provided by Dr. D. B. Steinman, M. ASCE.

4, 5, 6, 7. Footnotes in Proc. Sep. 558.

Table 6

Values of D_o or D_s

(1) $c\ell$	(2) $\frac{D_o EI}{f^2 \ell}$	(3) $D_o H_r \ell / f^2$ $= (2) \times c^2 \ell^2$	(1) $c\ell$	(2) $\frac{D_o EI}{f^2 \ell}$	(3) $D_o H_r \ell / f^2$	(1) $c\ell$	(2) $\frac{D_o EI}{f^2 \ell}$	(3) $D_o H_r \ell / f^2$
0	.53333	0	5.5	.13159	3.981	11	.040501	4.901
1.0	.48469	.485	6.0	.11514	4.145	12	.034465	4.963
1.5	.43451	.978	6.5	.10138	4.283	13	.029662	5.013
2.0	.37969	1.519	7.0	.08979	4.400	14	.025783	5.053
2.5	.32678	2.042	7.5	.07997	4.499	15	.022608	5.087
3.0	.27930	2.514	8.0	.07161	4.583	16	.019979	5.115
3.5	.23831	2.919	8.5	.06444	4.656	18	.015919	5.158
4.0	.20384	3.261	9.0	.05826	4.719	20	.012973	5.189
4.5	.17514	3.547	9.5	.05289	4.773	40	.003310	5.295
5.0	.15134	3.784	10.0	.04821	4.821	∞	0	5.333

Table 7

VALUES OF $H/_p\ell$ FOR ADVANCING UNIFORM LOAD

Values shown for ℓ = 10f and D = 1.25 D_o

For other proportions multiply tabulated values by 1.25 D_o/D x $\ell/10f$

K'/ℓ	$c\ell = 5$	$c\ell = 10$	$c\ell = 15$	K'/ℓ	$c\ell \leq 5$	$c\ell = 10$	$c\ell = 15$
.02	.0010	.0011	.0011	.28	.1842	.1870	.1887
.04	.0041	.0042	.0044	.30	.2090	.2117	.2134
.06	.0091	.0095	.0098	.32	.2350	.2376	.2392
.08	.0164	.0168	.0172	.34	.2620	.2644	.2659
.10	.0252	.0261	.0268	.36	.2897	.2922	.2933
.12	.0361	.0373	.0381	.38	.3182	.3204	.3215
.14	.0489	.0504	.0514	.40	.3476	.3494	.3504
.16	.0636	.0652	.0664	.42	.3774	.3788	.3797
.18	.0799	.0818	.0830	.44	.4075	.4088	.4095
.20	.0979	.1000	.1014	.46	.4381	.4390	.4395
.22	.1171	.1197	.1212	.48	.4688	.4693	.4697
.24	.1382	.1408	.1424	.50	.5000	.5000	.5000
.26	.1605	.1633	.1650	1.00	1.0000	1.0000	1.0000

Table 8

Values of $-c^2\ell^2 m_h/f$

$c\ell \backslash x$	0.1ℓ	0.2ℓ	0.3ℓ	0.4ℓ	0.5ℓ
3.0	1.842	3.126	3.969	4.445	4.599
3.5	2.195	3.672	4.611	5.133	5.302
4.0	2.519	4.150	5.156	5.701	5.873
4.5	2.817	4.567	5.609	6.161	6.331
5.0	3.092	4.932	5.987	6.529	6.695
5.5	3.346	5.250	6.300	6.824	6.981
6.0	3.584	5.530	6.560	7.059	7.205
6.5	3.808	5.780	6.778	7.245	7.380
7.0	4.014	6.001	6.961	7.393	7.517
8.0	4.400	6.373	7.244	7.606	7.706
9.0	4.746	6.672	7.447	7.745	7.824
10.0	5.056	6.916	7.594	7.831	7.892
11.0	5.337	7.112	7.701	7.891	7.934
12.0	5.590	7.272	7.779	7.928	7.960
13.0	5.820	7.405	7.837	7.952	7.976
14.0	6.024	7.512	7.880	7.968	7.984
15.0	6.213	7.602	7.911	7.979	7.991
16.0	6.385	7.674	7.934	7.986	7.994
18.0	6.678	7.782	7.964	7.994	8.000
20.0	6.920	7.854	7.980	8.000	8.000
40.0	7.854	7.998	8.000	8.000	8.000
∞	8.000	8.000	8.000	8.000	8.000

Tabular values may also be used to calculate $\eta_h = (y - m_h)/H_R$

Table 9 - CALCULATION OF BENDING MOMENTS

Point x/ℓ	.1	.2	.3	.4	.5
Main Span-Positive M, $c\ell = 14$					
(1) Load Position Figs. 16, 17, 18	$0-.26\ell$	$0-.33\ell$	$.11\ell-.43\ell$	$.25\ell-.53\ell$	$.37\ell-.63\ell$
(2) H_o - Table 7 x 3800 (kips)	625	944	1375	1490	1468
(3) $H_t + \delta H = -393-.0573\ H_o$ (kips)	-429	-447	-472	-478	-477
(4) m_h - Table 8 x $350/(14)^2$(ft)	-10.76	-13.42	-14.08	-14.22	-14.25
(5) M_i - Fig. 19 x $\overline{3800^2}/14$ (ft-kips)	44,600	49,400	44,100	40,100	39,100
(6) δM = (3) x (4)	4600	6000	6700	6800	6800
(7) M = (5) + (6) (ft-kips)	49,200	55,400	50,800	46,900	45,900
(8) M (Interpolated) (ft-kips)	50,400	56,000	51,200	47,000	46,100
Main Span - Negative M, $c\ell = 14$					
(9) H_o = 3800 - (2) (kips)	3175	2856	2425	2310	2332
(10) $2\ H_s + H_t + \delta H = 1101-.0573\ H_o$	924	938	963	970	968
(11) M_i (Fig. 20 x $\overline{3800^2}/14$) (ft-kips)	-33,330	-35,400	-29,520	-25,400	-24,340
(12) δM = (4) x (10) (ft-kips)	-9940	-12,600	-13,560	-13,800	-13,800
(13) M = (11) + (12) (ft-kips)	-43,270	-48,000	-43,080	-39,200	-38,140
(14) M (Interpolated) (ft-kips)	-40,200	-44,300	-40,300	-37,100	-36,000
Side Span - Positive M, $c_1\ell_1 = 6.45$					
(15) $m_h \times c_1^2\ell_1^2/f_1$ (Table 8)	3.786	5.755	6.756	7.226	7.363
(16) M (Eq. 72) = $5180 \times \frac{f_1}{c^2\ell^2} \times (15)$	36,900	56,000	65,900	70,400	71,800
Side Span - Negative M, $c_1\ell_1 = 7.05$					
(17) $m_h \times c_1^2\ell_1^2/f_1$ (Table 8)	4.033	6.023	6.975	7.404	7.532
(18) $M = Hm_h = 4640 \times f_1 / c_1^2\ell_1^2 \times (17)$	-29,600	-44,200	-51,100	-54,300	-55,200

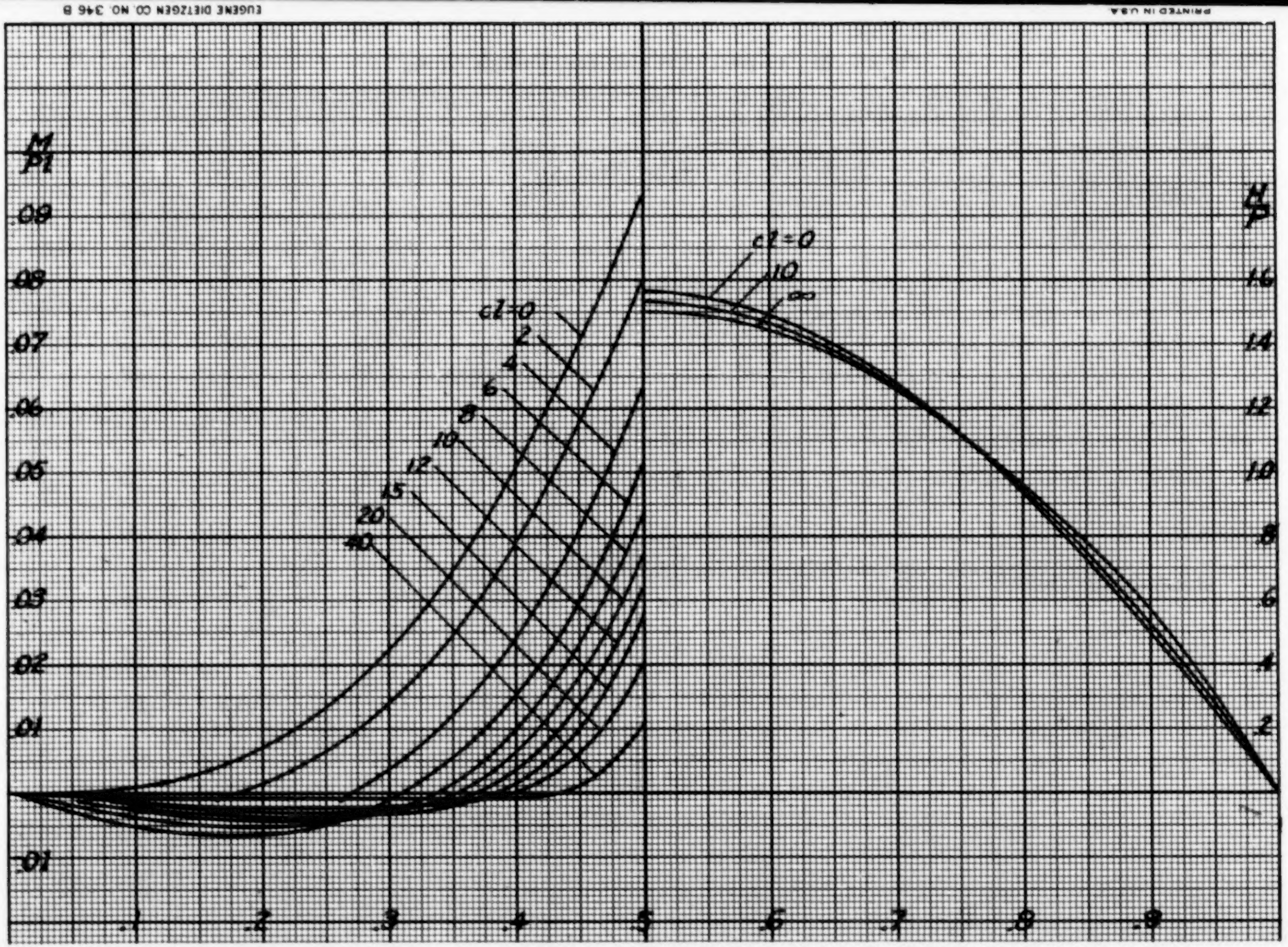

Fig. 16. Influence Lines for M at Mid-span (D = 1.25 D_0) and for H (D = 1.25 D_0, l = 10 f)

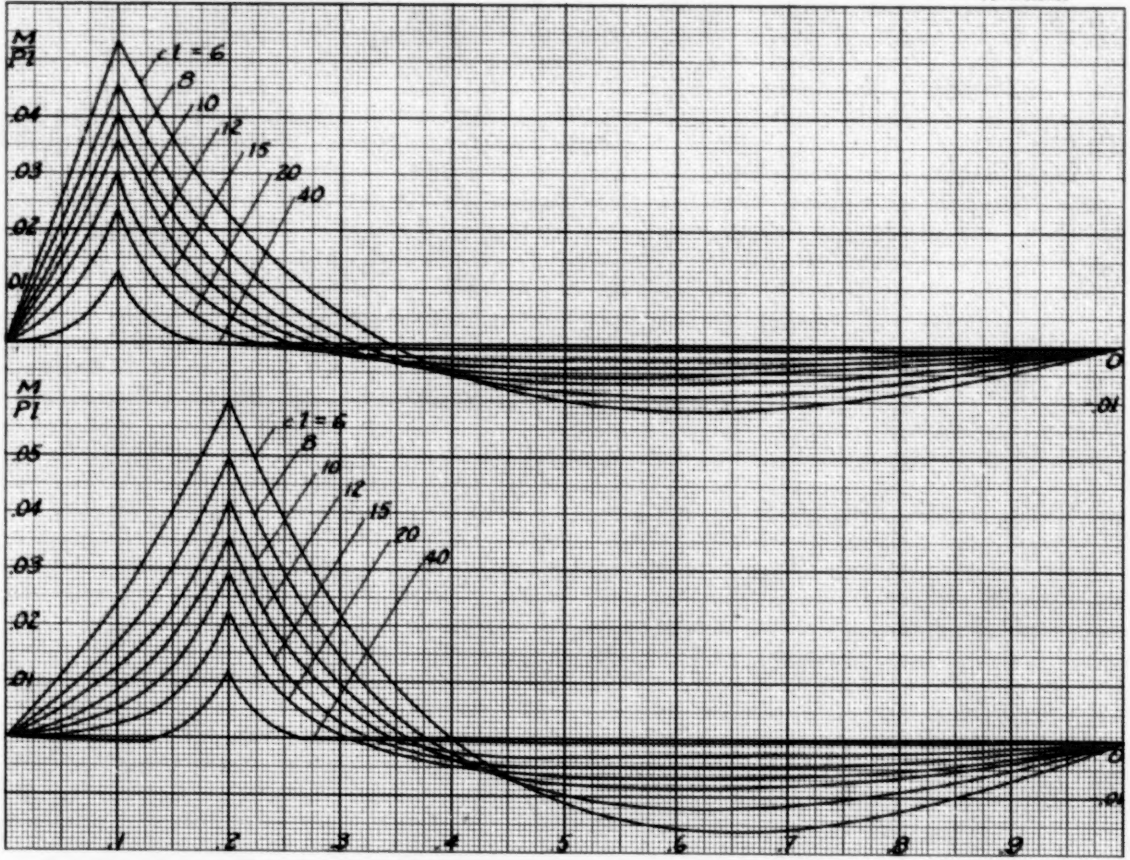

Fig. 17. Influence Lines for M at 0.1 l and 0.2 l (D = 1.25 D_0)

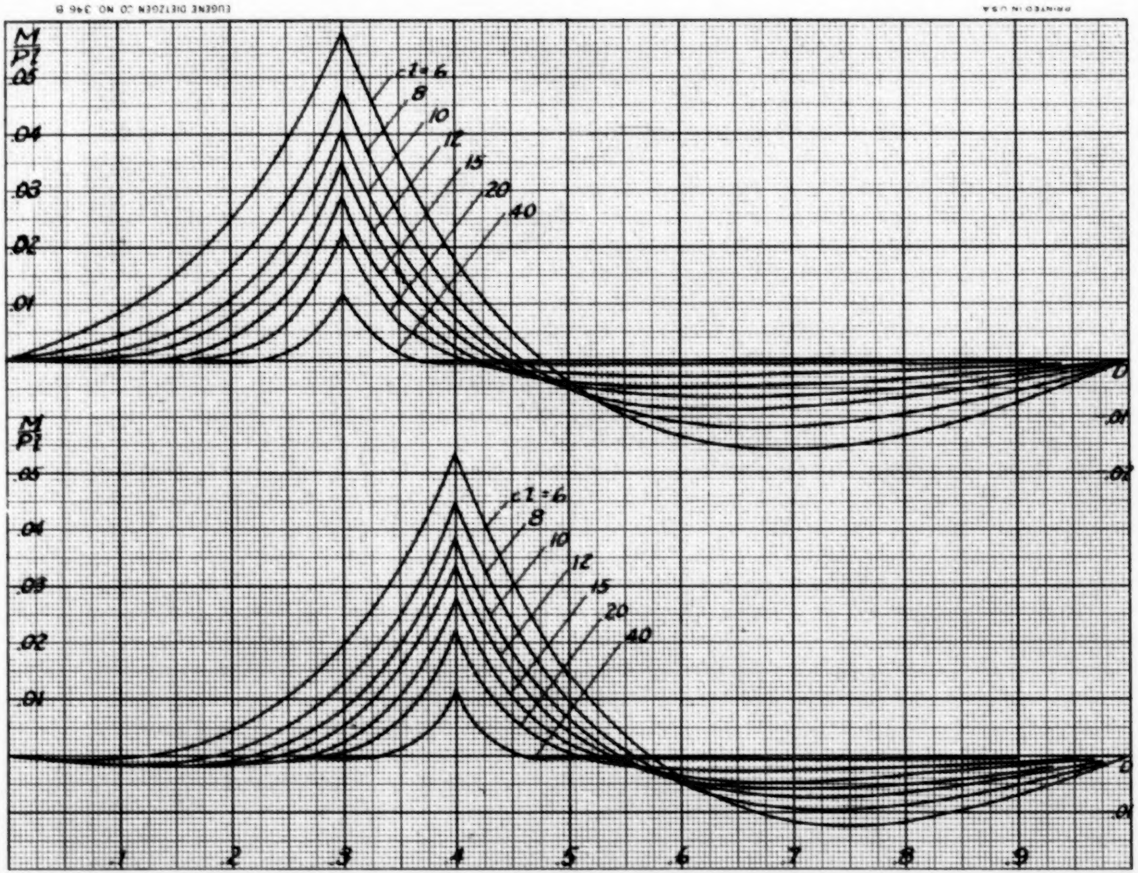

Fig. 18. Influence Lines for M at 0.3 l and 0.4 l (D = 1.25 D_0)

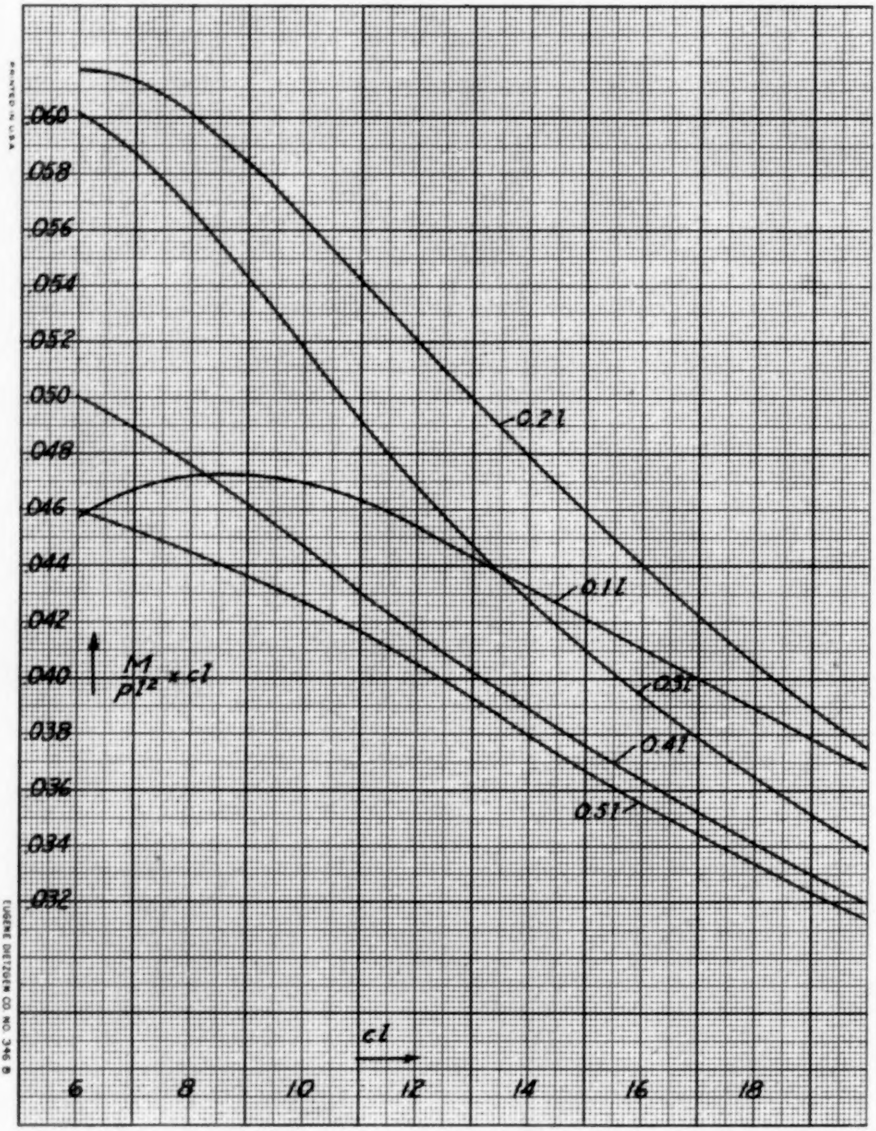

Fig. 19. Maximum Positive Bending Moments Resulting from Live Load in Main Span (D = 1.25 D_0)

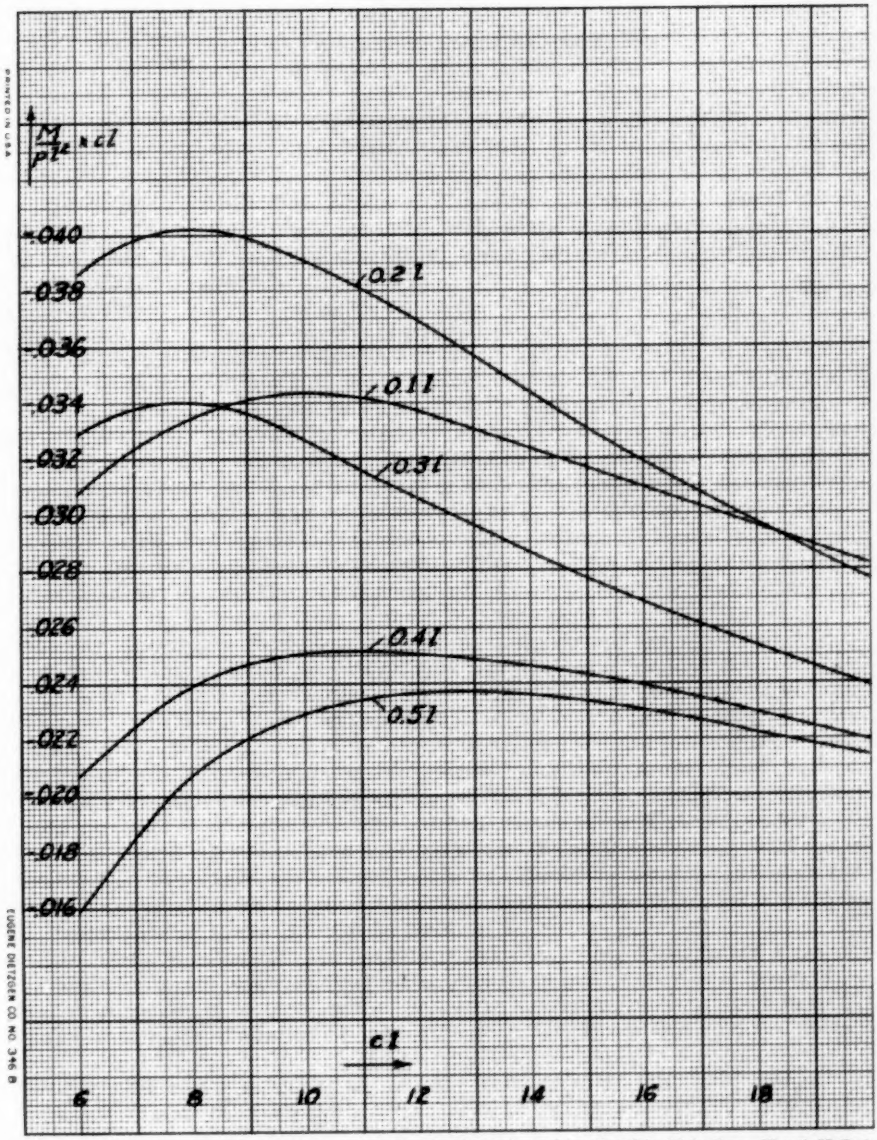

Fig. 20. Maximum Negative Bending Moments Resulting from Live Load in Main Span ($D = 1.25\ D_o$)

Discussion of
"ULTIMATE SLOPES AND DEFLECTIONS"
A Brief Limit for Design

by George C. Ernst
(Proc. Paper 583)

GEORGE C. ERNST,* M. ASCE.—Mr. Diwan's discussion is based in its entirety upon the rejection of the completely idealized relationship between M and ψ for conditions prior to collapse and a questioning of the value of the "unit rotation diagram."

With regard to the M and ψ relationship, the true curve is a function of steel ratio, local bond development and failure, steel properties in tension, and concrete properties in tension and compression. Up to initial tensile cracking not exceeding a unit deformation in the concrete of about 0.0002, a reinforced concrete beam does not materially differ from a plain concrete beam insofar as slope and deflection relationships are concerned. Subsequent to tensile cracking, the tensile properties of the concrete have a gradually decreasing effect until local failure of bond occurs between cracks, thereby resulting in steel deformations conforming to $E_s = 30{,}000{,}000$ psi over substantial portions of the beam. Crack formation during the early stages of loading does not produce accumulated rotations as calculated with an $E_s = 30{,}000{,}000$ psi as Mr. Diwan has assumed. From the development of yield in the steel at M_o to the ultimate moment M_u, the shape of the curve is dominated by the compression properties of the concrete and the steel ratio[10] for any given grade of steel. In general, progressive local bond failure in the vicinity of tensile cracks begins at a unit deformation of about 0.0002 in the concrete and a steel stress at the crack of about 15,000 psi. Figure 13 compares the M - ψ curves for three different assumptions as to the effective E_s, the intermediate one being most representative of the true variation. Figure 14 compares the slopes and deflections for a simply supported beam with concentrated load at midspan, for which the curvature from M_o to M_u in Mr. Diwan's Type 2 curve has been used with each of the three assumptions for effective E_s. Obviously, the assumption of an infinite E_s merely expresses the upper limit of stiffness for the tensile face, and the value of 30,000,000 psi for E_s expresses the lower limit up to yield.

Mr. Diwan's belief that the curvature from M_o to M_u will provide a realistic estimate of the length of the plastic portion in the vicinity of a "peaked" M_u for purposes of moment redistribution in a continuous structure can be shown to be quite unwarranted. Unfortunately, Mr. Diwan has selected relatively favorable conditions for redistribution of moments in his examples. However, taking the values of M_o and M_u from his table, the difference in moment is about 7% of M_u for a drop of 87% in unit rotation for AB, and 6.4% for a 93% drop for BC and CD. In the vicinity of a linearly peaked M_u, therefore, 7% (for AB) or 6.4% (for BC or CD) of the distance to zero moment on either side of M_u would be affected by the unit rotations between M_o and M_u.

---

* Prof. and Chairman, Dept. of Civ. Eng., Univ. of Nebraska, Lincoln, Nebr.

[10] "Inelastic Behavior of Reinforced Concrete Members subjected to Short-Time Static Loads," L. H. N. Lee, ASCE Proc.-Separate No. 286, 1953.

For Mr. Diwan's loading 2 on his single bay frame, the required length over which ψ_o to ψ_u must be accumulated to produce ϕ_c is 12.0 inches, whereas the length actually affected from M_o to M_u is only 6.4% of 120 inches or 7.7 inches. Apparently Mr. Diwan is depending upon some other unstated property to provide for the total required angle change. Figure 15 illustrates the effect of varying the steel ratio and concrete strength upon the minimum length over which plastic rotation must occur at the supports of a fixed end beam under uniform load in order to assure complete moment redistribution. It should be recalled that ψ markedly decreases when the steel ratio is increased or the concrete strength reduced,[11] thereby reducing the total angle change available for moment redistribution by virtue of the portion of the beam affected by M_o to M_u. Contrarily, this in turn increases the required minimum length of plastic hinging as is shown in Figure 15.

All this adds up to the fact that it should be reasonably obvious that moment redistribution cannot be significantly dependent upon the difference between Mr. Diwan's Type 1 and Type 2 curves in his Figure 8, but rather on the distribution of ψ_u as controlled by the distance throughout which steel yield can occur due to length of bearing, width of column, shape of knee, etc. The effect of these factors can be determined only by laboratory tests of full-sized members and structures.

As to the value of the "unit rotation diagram," it is undoubtedly realized by all readers that the M/EI diagram is a unit rotation diagram based upon a linear relationship between stress and strain. The M/EI concept for those portions of a structure below first yield was not presented because, for the purpose of the paper, it was felt best to avoid the obscuring of the purely geometrical relationship between deformations, slopes, and deflections. The author does not believe that the unit rotation diagram, either in its basic form or converted to M/EI form, will have any significant usage in ultimate load or limit design. It has a rather limited usefulness even for the so-called "elastic" method of analysis. The problem is essentially that of obtaining a fundamental understanding of structural response throughout the loading history of a structure, and a very necessary part of the problem is the experimental determination of the extent of distribution of unit rotations beyond first yield. The paper was intended to draw attention to this feature as well as the moment-slope-deflection relationship, and the author is indebted to Mr. Diwan for the opportunity of emphasizing its importance.

---

[11] Ibid. at 10.

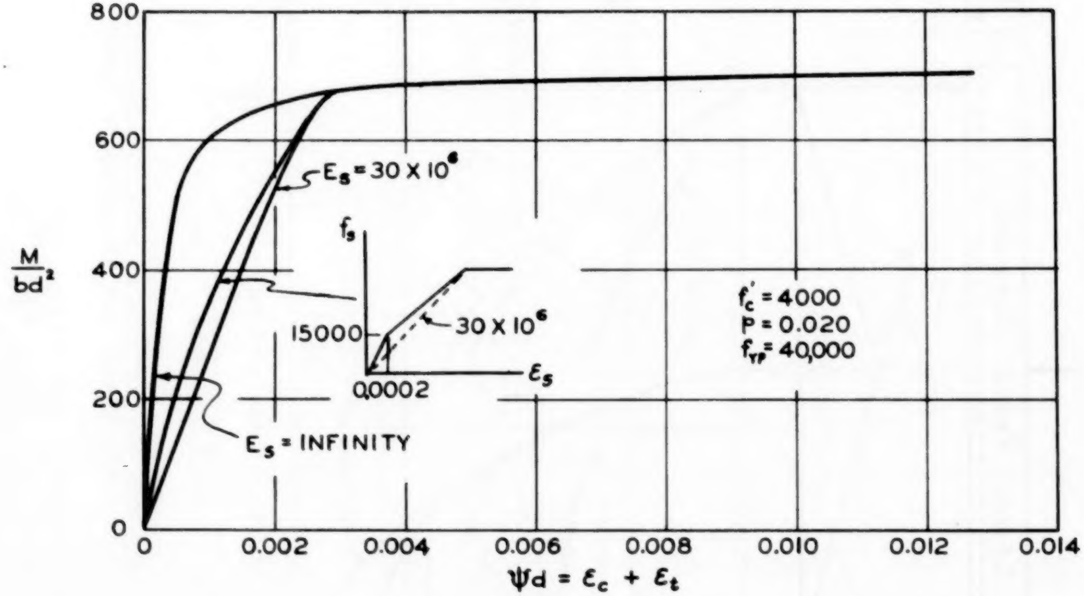

FIGURE 13. UNIT ROTATION AS AFFECTED BY REDUCTION IN STEEL STRAIN DUE TO CONCRETE COVER

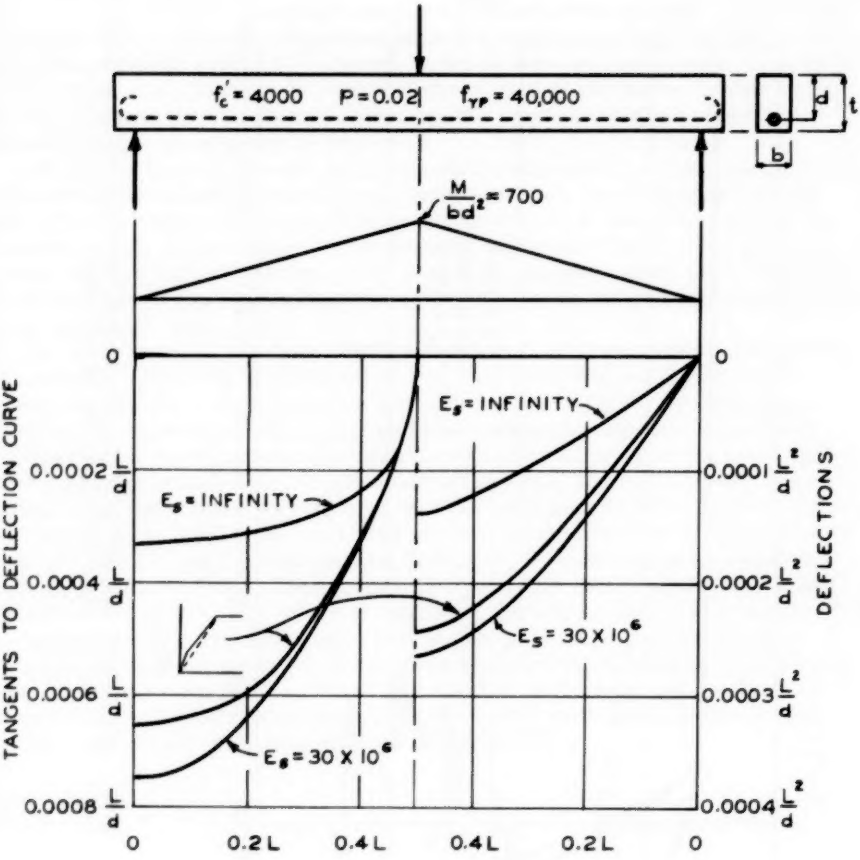

FIGURE 14. SLOPES AND DEFLECTIONS AS AFFECTED BY REDUCTION IN STEEL STRAIN DUE TO CONCRETE COVER

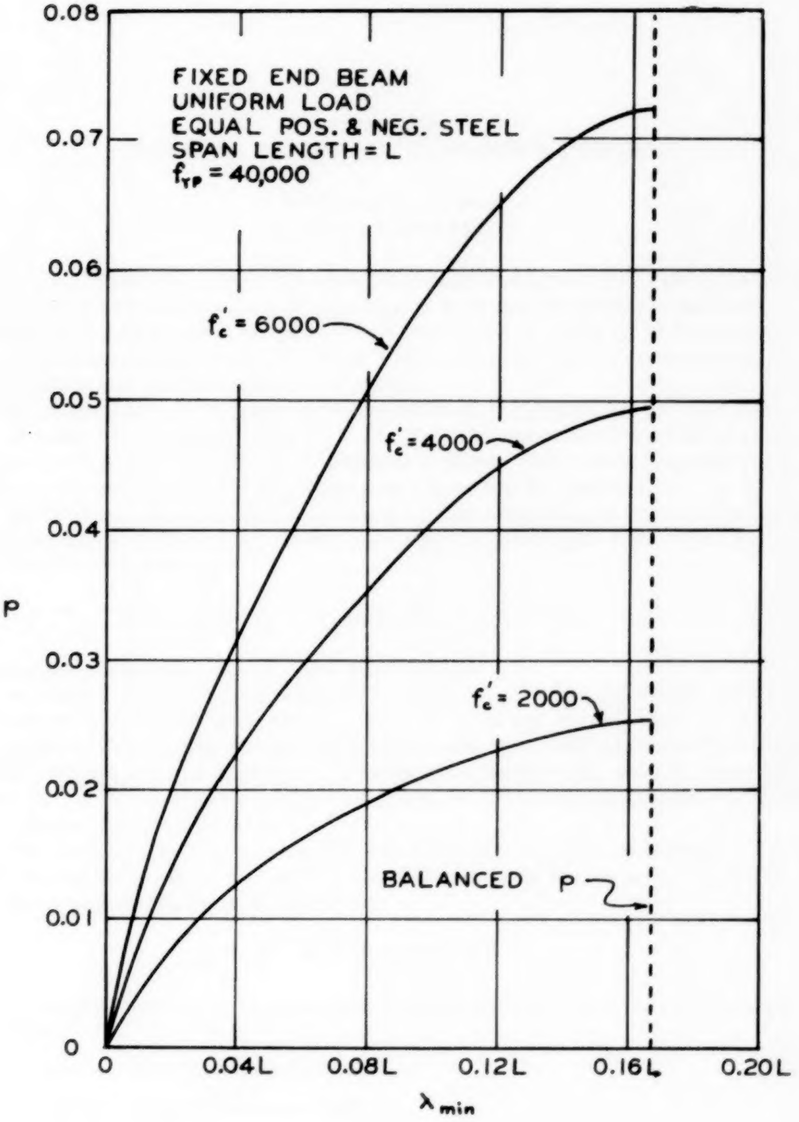

FIGURE 15. STEEL RATIO VS. MINIMUM LENGTH OF DISTRIBUTION (λ_{min}) FOR EQUAL POSITIVE AND NEGATIVE STEEL RATIOS.

Discussion of "LATERAL BENDING OF SUSPENSION BRIDGES"

by Cevdet A. Erzen

(Proc. Paper 663)

A. SELBERG.*—Since 1932, when Moisseiff and Lienhard(4) published their paper on the lateral bending of suspension bridges, this problem has been frequently handled in the literature.(5-10) However, already in 1906, an approximate solution was given by J. Melan(1), and description of a more exact investigation was given on the same place.

Investigations of the same problem were also given in 1919(2) and 1921.(3)

The very interesting paper by C. A. Erzen gives a method which may be used on all possible types of suspension bridges. The method is, however, laborious, and takes a lot of unnecessary time for the designer.

To get a quick and accurate solution of this problem, the best method is to express the horizontal component of tension in suspender ropes T as a series.(6) For instance

$$T = A_1 \sin\pi\frac{x}{l} + A_2 \sin 2\pi\frac{x}{l} + A_3 \sin\pi\frac{x}{l} + - - -$$

For symetrical spans A_2; A_4 etc. will be zero.

For smaller suspension bridges the terms A_1 or A_1 ; A_2 will be sufficient for all practical purposes, and for greater spans A_1; A_2; A_3 usually will be sufficient. Calculating the example used by Moiseiff and Lienhard(4) with the terms A_1; A_3 gives a difference in moments less than 2%, with 3 terms less than 1%. If T is expressed by a series u, M and v are found from equations (1), (3) and (5) by integration.

The simplest method for finding the coefficients in the series for T is to use the equation (4). The equation shall be satisfied for so many values of x as there are coefficients in the series.

BIBLIOGRAPHY

1. J. Melan. Handbuch d. Ingenieur Wissenschaften. II. 5. p. 257. Leipzig 1906.
2. N. Royen. Der Eisenbau 1919.
3. E. Melan. Der Brückenbau 1921.
4. L. S. Moisseiff a. F. Lienhard. Proc. A.S.C.E. 1932.
5. H. H. Bleich: Die Berechnung verankerter Hängebrücken. Wien 1935.
6. A. Selberg: Der Stahlbau 1941.
7. A. Selberg: Publications V. 7. Int. Ass. f. Bridge and Structural Eng. Zurich 1943/44.

---

* Prof., Theory of Structures, Norw. Technical Univ., Norway.

8. A. Aas - Jakobsen: Teknisk Tidskrift 1943.

9. O. F. Theimer: Der Bauigenieur 1941.

10. A. Selberg: Design of Suspension Bridges. K.N.V.S. Trondheim Norway 1946.

CEVDET A. ERZEN.*—The writer is much grateful to Dr. Selberg for his discussion of the problem of bending of suspension bridges under the effect of wind forces. The extensive literature on the problem as pointed out by Dr. Selberg is noteworthy.

It is interesting to see the method by which this problem is solved by using a finite trigonometric series. The method, known as the Collocation Method, has been used quite extensively in the solution of differential equations. However, it is necessary that each term of the series chosen for the purpose must approximate in shape the variation of the function that it represents. Otherwise convergence is not easily attained.

The trigonometric series recommended in the discussion is apparently one that gives very rapid convergence if, with only two terms, one can obtain results within two percent. Integration of Eqs. (1) and (3) with T expressed by a trigonometric series is a simple matter if p_t is constant throughout the span. However, it may take a considerable time to integrate p_t if it is a function of x as given in the example. In this case, the writer believes that using a finite trigonometric series approach is not a simpler way to solve the problem.

---

* Asst. Prof. of Civ. Eng., Cornell Univ., Ithaca, N. Y.

PROCEEDINGS PAPERS

The technical papers published in the past year are identified by number below. Technical-division sponsorship is indicated by an abbreviation at the end of each Paper Number, the symbols referring to: Air Transport (AT), City Planning (CP), Construction (CO), Engineering Mechanics (EM), Highway (HW), Hydraulics (HY), Irrigation and Drainage (IR), Power (PO), Sanitary Engineering (SA), Soil Mechanics and Foundations (SM), Structural (ST), Surveying and Mapping (SU), and Waterways (WW) divisions. Papers sponsored by the Board of Direction are identified by the symbols (BD). For titles and order coupons, refer to the appropriate issue of "Civil Engineering" or write for a cumulative price list.

VOLUME 80 (1954)

OCTOBER: 512(SM), 513(SM), 514(SM), 515(SM), 516(SM), 517(PO), 518(SM)[c], 519(IR), 520(IR), 521(IR), 522(IR)[c], 523(AT)[c], 524(SU), 525(SU)[c], 526(EM), 527(EM), 528(EM), 529(EM), 530(EM)[c], 531(EM), 532(EM)[c], 533(PO).

NOVEMBER: 534(HY), 535(HY), 536(HY), 537(HY), 538(HY)[c], 539(ST), 540(ST), 541(ST), 542(ST), 543(ST), 544(ST), 545(SA), 546(SA), 547(SA), 548(SM), 549(SM), 550(SM), 551(SM), 552(SA), 553(SM)[c], 554(SA), 555(SA), 556(SA), 557(SA).

DECEMBER: 558(ST), 559(ST), 560(ST), 561(ST), 562(ST), 563(ST)[c], 564(HY), 565(HY), 566(HY), 567(HY), 568(HY)[c], 569(SM), 570(SM), 571(SM), 572(SM)[c], 573(SM)[c], 574(SU), 575(SU), 576(SU), 577(SU), 578(HY), 579(ST), 580(SU), 581(SU), 582(BD).

VOLUME 81 (1955)

JANUARY: 583(ST), 584(ST), 585(ST), 586(ST), 587(ST), 588(ST), 589(ST)[c], 590(SA), 591(SA), 592(SA), 593(SA), 594(SA), 595(SA)[c], 596(HW), 597(HW), 598(HW)[c], 599(CP), 600(CP), 601(CP), 602(CP), 603(CP), 604(EM), 605(EM), 606(EM)[c], 607(EM).

FEBRUARY: 608(WW), 609(WW), 610(WW), 611(WW), 612(WW), 613(WW), 614(WW), 615(WW), 616(WW), 617(IR), 618(IR), 619(IR), 620(IR), 621(IR)[c], 622(IR), 623(IR), 624(HY)[c], 625(HY), 626(HY), 627(HY), 628(HY), 629(HY), 630(HY), 631(HY), 632(CO), 633(CO).

MARCH: 634(PO), 635(PO), 636(PO), 637(PO), 638(PO), 639(PO), 640(PO), 641(PO)[c], 642(SA), 643(SA), 644(SA), 645(SA), 646(SA), 647(SA)[c], 648(ST), 649(ST), 650(ST), 651(ST), 652(ST), 653(ST), 654(ST)[c], 655(SA), 656(SM)[c], 657(SM)[c], 658(SM)[c].

APRIL: 659(ST), 660(ST), 661(ST)[c], 662(ST), 663(ST), 664(ST)[c], 665(HY)[c], 666(HY), 667(HY), 668(HY), 669(HY), 670(EM), 671(EM), 672(EM), 673(EM), 674(EM), 675(EM), 676(EM), 677(EM), 678(HY).

MAY: 679(ST), 680(ST), 681(ST), 682(ST)[c], 683(ST), 684(ST), 685(SA), 686(SA), 687(SA), 688(SA), 689(SA)[c], 690(EM), 691(EM), 692(EM), 693(EM), 694(EM), 695(EM), 696(PO), 697(PO), 698(SA), 699(PO)[c], 700(PO), 701(ST)[c].

JUNE: 702(HW), 703(HW), 704(HW)[c], 705(IR), 706(IR), 707(IR), 708(IR), 709(HY)[c], 710(CP), 711(CP), 712(CP), 713(CP)[c], 714(HY), 715(HY), 716(HY), 717(HY), 718(SM)[c], 719(HY)[c], 720(AT), 721(AT), 722(SU), 723(WW), 724(WW), 725(WW), 726(WW)[c], 727(WW), 728(IR), 729(IR), 730(SU)[c], 731(SU).

JULY: 732(ST), 733(ST), 734(ST), 735(ST), 736(ST), 737(PO), 738(PO), 739(PO), 740(PO), 741(PO), 742(PO), 743(HY), 744(HY), 745(HY), 746(HY), 747(HY), 748(HY)[c], 749(SA), 750(SA), 751(SA), 752(SA)[c], 753(SM), 754(SM), 755(SM), 756(SM), 757(SM), 758(CO)[c], 759(SM)[c], 760(WW)[c].

AUGUST: 761(BD), 762(ST), 763(ST), 764(ST), 765(ST)[c], 766(CP), 767(CP), 768(CP), 769(CP), 770(CP), 771(EM), 772(EM), 773(SA), 774(EM), 775(EM), 776(EM)[c], 777(AT), 778(AT), 779(SA), 780(SA), 781(SA), 782(SA)[c], 783(HW), 784(HW), 785(CP), 786(ST).

SEPTEMBER: 787(PO), 788(IR), 789(HY), 790(HY), 791(HY), 792(HY), 793(HY), 794(HY)[c], 795(EM), 796(EM), 797(EM), 798(EM), 799(EM)[c], 800(WW), 801(WW), 802(WW), 803(WW), 804(WW), 805(WW), 806(HY), 807(PO)[c], 808(IR)[c].

OCTOBER: 809(ST), 810(HW)[c], 811(ST), 812(ST)[c], 813(ST)[c], 814(EM), 815(EM), 816(EM), 817(EM), 818(EM), 819(EM)[c], 820(SA), 821(SA), 822(SA)[c], 823(HW), 824(HW).

c. Discussion of several papers, grouped by Divisions.

AMERICAN SOCIETY OF CIVIL ENGINEERS

OFFICERS FOR 1955

PRESIDENT
WILLIAM ROY GLIDDEN

VICE-PRESIDENTS

Term expires October, 1955:	*Term expires October, 1956:*
ENOCH R. NEEDLES	FRANK L. WEAVER
MASON G. LOCKWOOD	LOUIS R. HOWSON

DIRECTORS

Term expires October, 1955:	*Term expires October, 1956:*	*Term expires October, 1957:*
CHARLES B. MOLINEAUX	WILLIAM S. LaLONDE, JR.	JEWELL M. GARRELTS
MERCEL J. SHELTON	OLIVER W. HARTWELL	FREDERICK H. PAULSON
A. A. K. BOOTH	THOMAS C. SHEDD	GEORGE S. RICHARDSON
CARL G. PAULSEN	SAMUEL B. MORRIS	DON M. CORBETT
LLOYD D. KNAPP	ERNEST W. CARLTON	GRAHAM P. WILLOUGHBY
GLENN W. HOLCOMB	RAYMOND F. DAWSON	LAWRENCE A. ELSENER
FRANCIS M. DAWSON		

PAST-PRESIDENTS
Members of the Board

WALTER L. HUBER **DANIEL V. TERRELL**

EXECUTIVE SECRETARY
WILLIAM H. WISELY

TREASURER
CHARLES E. TROUT

ASSISTANT SECRETARY
E. L. CHANDLER

ASSISTANT TREASURER
CARLTON S. PROCTOR

PROCEEDINGS OF THE SOCIETY

HAROLD T. LARSEN
Manager of Technical Publications

DEFOREST A. MATTESON, JR.
Editor of Technical Publications

PAUL A. PARISI
Assoc. Editor of Technical Publications

COMMITTEE ON PUBLICATIONS

SAMUEL B. MORRIS, *Chairman*

JEWELL M. GARRELTS, *Vice-Chairman*

GLENN W. HOLCOMB **OLIVER W. HARTWELL**

ERNEST W. CARLTON **DON M. CORBETT**